HHS Public Access

Author manuscript

*Bioconjug Chem*. Author manuscript; available in PMC 2023 September 21.

# Porous Silicon Nanoparticles Targeted to the Extracellular Matrix for Therapeutic Protein Delivery in Traumatic Brain Injury

**Lauren E. Waggoner**[a,‡], **Jinyoung Kang**[a,‡,†], **Jonathan M. Zuidema**[b,c,‡], **Sanahan Vijayakumar**[b], **Alan A. Hurtado**[d], **Michael J. Sailor**[a,b,d], **Ester J. Kwon**[d,*]

[a]Department of Nanoengineering, University of California, San Diego, La Jolla, CA, 92093, USA

[b]Department of Chemistry & Biochemistry, University of California, San Diego, La Jolla, CA, 92093, USA

[c]Department of Neuroscience, University of California, San Diego, La Jolla, CA, 92093, USA

[d]Department of Bioengineering, University of California, San Diego, La Jolla, CA, 92093, USA

## Abstract

Traumatic brain injury (TBI) is a major cause of disability and death among children and young adults in the United States, yet there are currently no treatments that improve the long-term brain health of patients. One promising therapeutic for TBI is brain-derived neurotrophic factor (BDNF), a protein that promotes neurogenesis and neuron survival. However, outstanding challenges to the systemic delivery of BDNF are its instability in blood, poor transport into the brain, and short half-life in circulation and brain tissue. Here, BDNF is encapsulated into an engineered, biodegradable porous silicon nanoparticle (pSiNP) in order to deliver bioactive BDNF to injured brain tissue after TBI. The pSiNP carrier is modified with the targeting ligand CAQK, a peptide that binds to extracellular matrix components upregulated after TBI. The protein cargo retains bioactivity after release from the pSiNP carrier, and systemic administration of the CAQK-modified pSiNPs results in effective delivery of the protein cargo to injured brain regions in a mouse model of TBI. When administered after injury, the CAQK-targeted pSiNP delivery system for BDNF reduces lesion volumes compared to free BDNF, supporting the hypothesis that

*Address correspondence to ejkwon@ucsd.edu.

†Current Address: McGovern Institute for Brain Research, Massachusetts Institute of Technology, MA, 02139, USA

The manuscript was written through contribution of all authors. All authors have given approval to the final version of the manuscript.

‡These authors contributed equally

SUPPORTING INFORMATION

Schematic of protein loading, amination, PEG modification, and peptide modification of pSiNPs (Figure S1)

Representative TEM images at 25 kX and 50kX (scale bar = 200 nm) of pSiNPs, protein loaded pSiNPs, and protein loaded pSiNPs that are surface modified with PEG and CAQK (Figure S2)

Representative NISSL-stained coronal brain sections (Figure S3)

CONFLICT DISCLOSURE

MJS is a scientific founder (SF), member of the Board of Directors (BOD), Advisory Board (AB), Scientific Advisory Board (SAB), acts as a paid consultant (PC) or has an equity interest (EI) in the following: Aivocode, Inc (AB, EI); Bejing ITEC Technologies (SAB, PC); Cend Therapeutics (SF, BOD, EI); Illumina (EI); Matrix Technologies (EI); NanoVision Bio (SAB, EI); Pacific Integrated Energy (AB, EI); Quanterix (EI); Spinnaker Biosciences, Inc. (SF, BOD, EI); TruTag Technologies (SAB, EI); and Well-Healthcare Technologies (SAB, PC). MJS is also a Guest Professor at Zhejiang University, China. Although one or more of the grants that supported this research has been identified for conflict of interest management based on the overall scope of the project and its potential benefit to the companies listed, the research findings included in this publication may not necessarily relate to their interests. The terms of these arrangements have been reviewed and approved by the University of California, San Diego in accordance with its conflict of interest policies.

pSiNPs mediate therapeutic protein delivery after systemic administration to improve outcomes in TBI.

## Graphical Abstract

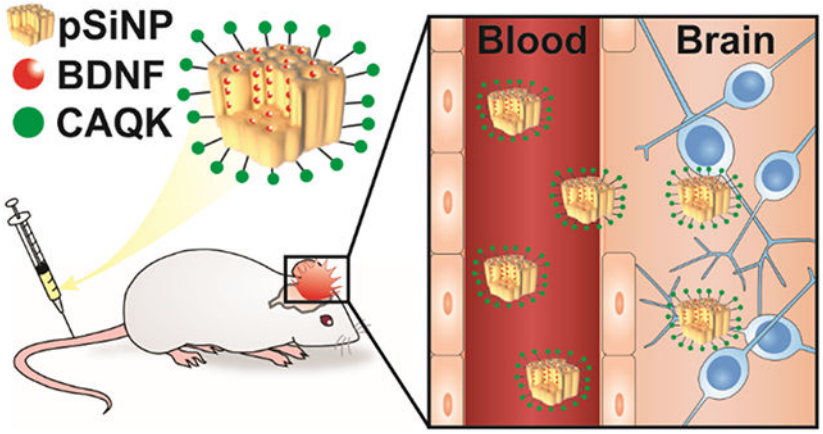


### Keywords

Brain Derived Neurotrophic Factor; Brain Targeting; Peptide Targeting; Nanomedicine; Systemic Delivery

## INTRODUCTION

Traumatic brain injury (TBI) results in up to 2.8 million injury-related hospitalizations and deaths in the United States annually.[1] Currently available treatments for TBI are palliative and do not address the underlying cause of disease, leading to long-term physical, behavioral, and/or psychosocial impairments in the majority of survivors.[2,3] After the initial injury, a secondary injury progresses over a course of days to weeks and the pathophysiology involves a series of biochemical and cellular cascades, including reactive oxygen species (ROS) generation, inflammatory response, neurodegeneration, blood-brain barrier (BBB) breakdown, and cell death.[4] While the primary injury can only be prevented, the secondary injury is an opportunity for therapeutic intervention in order to preserve brain tissue proximal to the primary injury.

Brain-derived neurotrophic factor (BDNF) is a promising neuroprotective therapeutic to mitigate the progressive deterioration of brain tissue that occurs during the secondary injury after TBI.[5] BDNF is a protein secreted from neurons and glia that promotes neuronal survival, neural plasticity, and neurogenesis[6,7] and its cognate receptor is tropomyosin receptor kinase B (TrkB).[8] TrkB activation initiates signaling cascades that regulate apoptosis, neuronal plasticity, and neurogenesis.[9] The binding of BDNF to TrkB activates pro-survival pathways and enhances expression of anti-apoptotic proteins through the phosphoinositide 3-kinase and Akt signaling pathway in neurons.[5,10] Previous studies have demonstrated that sustained BDNF levels in the brain achieved through stem cells,[11,12] genetically engineered cells,[13-18] viral gene therapy, and direct brain infusions[19] can

protect brain tissue in the context of nervous system injury, neurodegenerative disease, and psychiatric disorders.[5] In a meta-analysis of available clinical data, including cohort studies and randomized controlled trials, treatment of TBI patients with cerebrolysin, a porcine-derived peptide mixture that includes BDNF,[20] led to improved outcomes in functional tests such as the Glasgow Outcome Scale and modified Rankin Scale.[21] The promise of BDNF as a potential therapeutic for neurodegenerative diseases is highlighted by the initiation of a first-in-human clinical trial to evaluate adeno-associated virus vector (AAV2)-based gene therapy of BDNF in Alzheimer's Disease patients (NCT05040217).[22]

While elevated BDNF expression, along with other neurotrophic factors, contributes to the functional preservation of injured tissue, a major barrier to the development of BDNF as a clinical therapeutic for TBI is successful delivery to the injured brain after systemic administration. Challenges to intravenous delivery of BDNF include short circulation half-life and restricted transport into the brain.[5,23,24] Nanoscale drug delivery vehicles are platform technologies with the potential to increase the bioavailability and stability of protein therapeutics; for example, vehicles can be engineered to target specific tissues to increase retention and labile cargos can be encapsulated within the interior of vehicles to protect against degradation in the biological milieu.[24,25] In addition, the pharmacokinetic profiles of nanoscale drug delivery vehicles can be tuned independent of their therapeutic cargo, allowing for more facile formulation of a variety of cargos. However, previous efforts to encapsulate BDNF into nanoparticles have resulted in low mass loading of less than 1%.[26-28]

Porous silicon nanoparticles (pSiNPs) are an attractive candidate nano-carrier for therapeutics due to their tunable pore sizes and versatile loading chemistries, which allow for the accommodation of therapeutic cargo with a wide range of sizes and chemical properties, including small molecule drugs,[29,30] nucleic acids,[31-33] and peptides/proteins.[34,35] In particular, sequestration of protein-based biologics within the porous nanostructure of pSiNPs has been shown to protect them from degradation in the blood, leading to extended *in vivo* half-life and bioactivity.[29,32,34-44] In addition, pSiNPs have the advantage of linear degradation profiles, and thus can achieve linear drug release profiles, due to their anisotropic degradation mechanism.[45] This strategy has been successfully employed to encapsulate nerve growth factor (NGF) into pSiNPs, demonstrating the local release of growth factors from a polymeric scaffold.[34,38] In addition, Segal and Shefi et al. demonstrated neurotrophic factor release from nanoporous silicon microparticles after local delivery to the brain, achieved through the implantation of chips or biolistic bombardment using a pneumatic gene gun through an opening in the skull.[46] However, so far, protein delivery from pSiNPs after systemic delivery has yet to be demonstrated.

While a subset of TBI patients may undergo surgical intervention to remove blood clots and relieve intracranial pressure,[47] the brain is generally not readily accessible to therapeutics. Although intravenously delivered materials can accumulate in the injured brain through the damaged BBB that is a hallmark of TBI,[48-51, 52] access to the brain is transient, with a majority of materials excluded from the brain 6 hours after injury as the BBB rapidly re-establishes.[33,48,49] This highlights the need for active targeting strategies, in order to increase penetration and retention of potential therapeutics. We recently identified a

peptide ligand, CAQK, that binds to extracellular matrix (ECM) components upregulated after brain injury.[33] CAQK-modified pSiNPs were able to deliver siRNA to brains in a penetrating TBI model after intravenous administration and mediated significant silencing of a reporter protein compared to control targeted pSiNPs.[33] This approach exploited the transient damage to the BBB caused by the injury to allow passive accumulation of the nanoparticles into brain tissue where they selectively bound to, and were retained by, accessible brain ECM.

This work combines the above two approaches for protein loading and peptide-mediated targeting of ECM in the injured brain. Here we load BDNF into pSiNPs with a loading efficiency of 13% by mass of the pSiNP-protein construct, a substantial improvement in mass loading compared to encapsulation of BDNF by other systems (<1%),[26-28] and then modify the exterior of the nanoparticles with polyethylene glycol (PEG) and the brain injury-targeting peptide CAQK. We confirm that the BDNF retains its bioactivity after loading, we track the CAQK-modified pSiNPs into injured brain tissue after systemic administration in a mouse model of TBI, and we demonstrate a substantial reduction of brain lesion volumes relative to free BDNF or PBS controls. This work therefore represents the first time chemically-targeted nanoporous silicon has achieved the delivery of protein payloads after systemic administration and improved outcomes in an animal model of TBI.

## RESULTS AND DISCUSSION

### Loading of pSiNPs with Protein Cargo and Surface Modification with Targeting Peptide.

The pSiNPs used in this study were synthesized by electrochemical etching of mesopores into single crystalline silicon wafers, followed by ultrasonic fragmentation to form mesoporous nanoparticles. The electrochemical etch parameters (48% hydrofluoric acid, 46 mA/cm$^2$) were set to achieve a nominal pore size in the range of 10-20 nm in diameter and an average size of ~130 nm in hydrodynamic diameter (Figure 1).[45] The pore diameter was chosen based on previous studies to be sufficient to accommodate protein cargos.[45] The proteins were loaded into the pores of pSiNPs using an oxidative trapping method (Figure 1a,S1),[34,38] which involves partial conversion of the Si skeleton in pSiNPs to $SiO_2$ by mild oxidation in deionized water. The $SiO_2$ shell then re-structures in the presence of the aqueous protein solution. This combination of conversion of Si to $SiO_2$ and aqueous restructuring of $SiO_2$ results in a volume expansion of the skeleton and sealing of the protein within a hydrated silicate framework, effectively trapping the protein and protecting it from degradation in the blood upon systemic delivery. We studied two protein cargoes in this work: the therapeutic protein BDNF, and the model protein lysozyme, which was labeled with Rhodamine B. Lysozyme has a molecular weight of 14.5 kDa and an isoelectric point of 11.35[53] and BDNF has a molecular weight of 13.5 kDa and an isoelectric point between 9 and 10,[54] making their size and charge properties similar at physiologic pH, which are important parameters to consider for pSiNP protein loading. Rhodamine B-labeled lysozyme provides an established functional readout of protein activity in release assays and allows tracking of the payload by image analysis in the biodistribution studies. BDNF was used in efficacy studies in SH-SY5Y cultures and the animal model of TBI. The $SiO_2$ shell in the pSiNPs is negatively charged at physiologic pH, with a zeta potential ranging from −24

to −28 mV,[32] which enhanced the loading of the positively charged protein cargoes *via* electrostatic interactions (pI of lysozyme = 11.35[53] and pI of BDNF ~ 9-10[54]).

In order to verify surface modification and protein loading, we analyzed the pSiNPs by Fourier-transform infrared spectroscopy (FTIR), dynamic light scattering (DLS), and transmission electron microscopy (TEM) at each stage of synthesis. After oxidation and protein loading, the FTIR spectrum revealed characteristic amide I and II bands (at 1650 $cm^{-1}$ and 1530 $cm^{-1}$, respectively), denoting the presence of protein (Figure 1b).[55] Size measurements of unloaded pSiNPs and protein-loaded pSiNPs taken by DLS and TEM indicated that the loading process resulted in a diameter increase of ~5-10 nm, likely due to protein adsorption onto the pSiNP surface (Figure 1c,d,S2). To increase *in vivo* half-life and stability in systemic circulation,[56,57] the pSiNP surface was then aminated and modified with polyethylene glycol using NHS chemistry. PEG modification stabilized the nanoparticles, allowing them to be administered intravenously. To increase the retention of nanoparticles in the injured brain tissue, the pendant PEG groups were then conjugated to CAQK, a peptide previously discovered to bind upregulated proteoglycan complexes in injured brain tissue.[33] CAQK was attached to the distal end of PEG by reacting the free thiol of CAQK with a maleimide on the PEG. For some of the fluorescence imaging experiments, a FAM-labeled CAQK peptide was used. The surface chemistry was confirmed by FTIR; in particular, the appearance of a C-H stretching peak (2869 $cm^{-1}$) confirmed successful PEG conjugation.[58] The absolute diameter of the nanoparticles increased by ~10-20 nm after PEG and CAQK surface modification, while hydrodynamic diameter measurements increased by ~20-30 nm, likely due to the size increase in the hydrated shell around the nanoparticle after PEG modification (Figure 1c,d,S2). This size increase is consistent with the ~10 nm Flory radius of 5 kDa PEG and peptide.[59] Approximate number of peptides conjugated per pSiNP was found to be ~40,000-50,000 peptides per nanoparticle, as evaluated by quantifying the amount of FAM-labeled CAQK by absorbance and estimation of nanoparticle number by Nanoparticle Tracking Analysis. The zeta potential after surface modification of the protein-loaded pSiNPs containing the pendant PEG and CAQK groups was −1 ± 1.5 mV in PBS.

## Model Protein Cargo is Released Linearly from pSiNPs and Retains Activity.

Due to the high cost of BDNF, protein loading and performance parameters of the nanoparticle system were initially optimized using lysozyme as a model protein cargo. The degradation of pSiNPs is anisotropic due to the vertical pore orientation created by electrochemical etching that results in an increased surface area in the horizontal plane.[45] Silicon dioxide hydrolyses and dissolves in aqueous conditions to form biocompatible orthosilicic acid, releasing the protein payload during this process.[45] pSiNP-Lysozyme-PEG-CAQK were degraded in PBS and imaged with TEM over 48 hours, revealing a reduction in total nanoparticle size over time (Figure 2a). Lysozyme loading was quantified to be 14.5% by mass relative to the pSiNP-protein construct, measured by fully degrading pSiNPs in PBS at 37°C and measuring protein content with a BCA assay (Figure 2b). Next, we quantified the activity of the protein released from degraded pSiNPs. Lysozyme activity after release from pSiNPs was assayed in a Micrococcus lysodeikticus cell assay (Figure 2c). Lysozyme hydrolyzes the cell wall of M. lysodeikticus, which can be

monitored by decreased absorbance measured at 450 nm.[60] The combination of total protein measurements (Figure 2b) and protein activity (Figure 2c) confirmed that >95% of the protein released maintained its activity.

## CAQK Peptide-Targeted pSiNPs Mediate Protein Delivery into the Injured Brain after Systemic Administration.

In this work we employed the peptide CAQK as a targeting ligand for the nanoparticles. CAQK has been shown to bind to the ECM upregulated in injured brain tissue, and to selectively enhance nanoparticle accumulation in the damaged regions of the mouse brain.[33] We and others have demonstrated that intravenous delivery of targeted pSiNPs successfully led to accumulation and retention of cargo in target tissues, such as siRNA against STAT3 in breast cancer tumors[61] and siRNA against peptidylprolyl isomerase B[62] or green fluorescence protein in the injured brain.[33] Concerning biodegradation of the material, prior work has demonstrated that pSiNPs accumulate mostly within the liver and spleen after intravenous administration and degrade into orthosilicic acid in organs within 1-4 weeks.[29] Orthosilicic acid is naturally found in many tissues and excreted renally.[63] Previous studies of *in vivo* degradation of pSiNPs after intravenous administration found that degradation profiles approximate zero-order release,[64,65] similar to the linear release profile we observe (Figure 2b). Intravenously delivered pSiNPs are well-tolerated in mice up to 20 mg/kg.[29] In the present studies, the protein-loaded pSiNP formulations were administered at 5 mg/kg of pSiNP.

Controlled cortical impact (CCI) is a well-studied model of TBI in mice and the injury is created by performing a craniotomy and impacting the exposed dura with an electromagnetically-driven piston.[66] To determine if the targeted pSiNPs could deliver a protein cargo to the injured brain tissue after CCI, pSiNPs were synthesized with the model protein, Rhodamine B-labeled lysozyme. CAQK-targeted pSiNPs carrying this payload were administered intravenously 2 hours post-injury in mice given a CCI on the right hemisphere and brains were harvested 2 hours after injection (Figure 2d). The intrinsic luminescence from the quantum-confined silicon domains in the pSiNPs was imaged with time-gated imaging, which highlights the long-lived (microseconds) excited state of silicon quantum dots while suppressing short-lived (nanoseconds) tissue autofluorescence.[67] The time-gated images revealed the presence of intact pSiNPs in the injured hemisphere of the brain after systemic administration (Figure 2e). Brains were then sectioned and imaged by confocal microscopy to determine distribution of injected materials within the tissue (Figure 2f). We observe co-localization of fluorescent signal from Rhodamine B-labeled lysozyme and FAM-CAQK in the injured brain, surrounded by fluorescent signal from FAM-CAQK in adjacent areas. We believe that the FAM-CAQK fluorescent signal not co-localized with Rhodamine B-labeled lysozyme is due to surface degradation of pSiNPs, thus liberating FAM-CAQK that can subsequently diffuse into the surrounding tissue. These results support the hypothesis that CAQK-targeted pSiNPs can accumulate in the injured brain and deliver protein cargos after systemic administration. This result is consistent with previous studies of CAQK-targeted pSiNPs carrying siRNA cargo in a penetrating brain injury model, where CAQK- but not CGGK control-modified pSiNPs mediated gene silencing in the injured brain tissue.[33]

### BDNF is Released Linearly from pSiNPs over 72 Hours and Maintains Activity.

BDNF loading was determined by ELISA to be 13.3 ± 0.7% by mass relative to the total construct and complete degradation of the pSiNP-BDNF construct occurred over 72 hours in PBS at 37 °C (Figure 3a). To confirm that BDNF released from pSiNPs maintained activity, we performed a functional assay of the pSiNP-BDNF constructs in SH-SY5Y cultures, a human neuroblastoma cell line, which were differentiated with retinoic acid to induce the expression of TrkB, the receptor for BDNF.[68,69] Improved cell viability and neurite extension are well-established responses to BDNF treatment in SH-SY5Y cultures expressing TrkB.[69-71] The pSiNP-BDNF and free BDNF-treated cultures exhibited significantly increased cell viability with treatment in a dose-dependent manner compared to untreated and empty pSiNP-treated cultures, which had no effect on cell viability even at their highest dose (Figure 3b). Free BDNF-treated cultures displayed higher cell viability at most doses compared to pSiNP-BDNF-treated cultures, likely due to the immediate availability of free BDNF in *in vitro* conditions (Figure 3a,b). Imaging of cultures for morphological changes revealed that free BDNF and pSiNP-BDNF treatments increased presence of fine and complex neurites, with multiple crossing points, and a lower density of cytoskeletal actin surrounding the nucleus compared to control and pSiNP treatments (Figure 3c). The similar release profiles of lysozyme and BDNF (Figure 2b, 3a) and the preservation of activity observed with the released lysozyme (Figure 2c) and the released BDNF (Figure 3b,c) support the hypothesis that the protein cargos retain their biological activity in the pSiNP formulations.

BDNF is a growth factor with pleiotropic functions known to improve neuron survival, synaptic function, and cell signaling in animal models of injury and neurodegeneration.[5] Previous studies have demonstrated that elevated BDNF concentrations in the brain achieved through stem cell engraftment increased the expression of synaptic proteins and improved neurological scores in murine models of TBI.[11,72-74] Due to the numerous challenges with cell therapy, alternative approaches that enable the systemic delivery of recombinant BDNF protein are desired.

The half-life of BDNF is reported to be <10 minutes in plasma[75,76] and ~3 hours in brain tissue.[77] This very short time window illustrates the challenge of developing BDNF, and protein-based biologics in general, as systemically administered therapeutics. The use of a nanoparticle carrier in order to protect and increase bioavailability of BDNF in the brain after systemic administration has therefore been considered by several researchers as a potential solution to this problem. Of particular relevance to the present work, a previous report of nanoparticle-mediated delivery of BDNF employed poly(lactic-co-glycolic acid) (PLGA) nanoparticles.[78] This PLGA nanoparticle formulation of BDNF improved neurological behavior scores over free BDNF, supporting the potential benefit of BDNF delivered by nanoparticles.[78] In this prior work, BDNF was adsorbed onto the surface of the PLGA nanoparticles, likely due to the known challenge of maintaining protein activity when encapsulating protein drugs into the core of PLGA nanoparticles. In addition to the denaturing property of polymers and polymer surfaces, surface adsorption has a limited loading capacity, it usually displays burst release kinetics, and it leaves the biologic exposed to potential degradation by proteolytic enzymes. By comparison, the present approach

preserves protein activity (Figures 2c, 3b,c), can achieve high mass loading (~13 wt%) to enhance potency, and it yields zero-order release kinetics (Figures 2b, 3a).

### Treatment with pSiNP-BDNF Reduces Lesion Volumes in a Mouse Model of TBI.

After CCI, there is progressive loss of tissue due to secondary injury mechanisms that results in a lesion,[79-81] including neuronal cell death which peaks 24-72 hours after the primary injury.[82,83] The volume of this lesion correlates with functional deficits such as motor activity and memory.[84,85] In order to evaluate the therapeutic potential of pSiNP-BDNF after systemic delivery, we administered pSiNPs *via* the tail-vein in a mouse CCI model of TBI and measured lesion volume three days post-injury (Figure 4a). Mice were injured on the right hemisphere of the brain with a CCI, and CAQK-targeted pSiNPs carrying BDNF were administered through the tail-vein 2 hours post-injury (5 mg/kg pSiNP and 0.65 mg/kg BDNF). Controls included animals that received PBS, empty pSiNPs with PEG-CAQK (5 mg/kg), or free BDNF (1 mg/kg). While our previous work demonstrated the improved accumulation of CAQK-targeted pSiNPs compared to control-targeted pSiNPs,[33] a limitation of the current study is that we do not evaluate the impact of CAQK-targeting on pSiNP-BDNF accumulation. Three days after injury, brains were harvested and serial coronal sections were collected every 0.5 mm across the injury lesion (11-12 sections per brain). Lesion area was measured from each section and the lesion volume calculated by the trapezoidal rule, as described previously.[81,86,87] Nissl staining of neuronal cell bodies supported the presence of neurons in the area surrounding the injury in all groups (Figure S3), suggesting that any neurons that died during primary or secondary injury were included in the lesion area. We observed a 24.0% reduction in lesion volume in pSiNP-BDNF treated mice compared to the PBS treated control group (Figure 4b,c). In comparison, lesion volumes in free BDNF treated mice were equivalent to lesion volumes in the PBS control. We hypothesize that the reduction in lesion volume in pSiNP-BDNF treated mice is due to the ability of pSiNPs to localize to injured brain tissue (Figure 2e,f) and release active BDNF over a period of time (Figure 3) that is consistent with peak neuronal apoptosis.[82,83]

Lesion volumes in mice treated with empty pSiNPs (CAQK-targeted without BDNF) were reduced by 12.8% compared to the control PBS treatment ($p = 0.58$). pSiNPs and their degradation product silicic acid are known to interact with calcium ions, forming calcium silicate,[31] and ROS, which catalyzes the oxidation of porous silicon during its degradation process.[65] Calcium and ROS levels are elevated in the brain microenvironment after TBI as part of the damaging biochemical pathways that make up secondary injury.[88-90] However, more extensive studies on the interaction of pSiNPs with the injured brain microenvironment are needed to be able to draw conclusions about the extent or nature of the effect observed in animals administered empty pSiNPs.

## CONCLUSIONS

While therapeutic proteins are attractive candidates to address the complicated disease biology of TBI, the systemic delivery of proteins for treatment of TBI is challenging due to the instability of proteins in the blood and limited transport into the brain.[5,23,24,91] This work demonstrated a peptide-targeted pSiNP platform that addressed these challenges. We found

that up to 13% by mass of the BDNF protein could be loaded into the pores of pSiNPs, and measurement of cell viability in retinoic acid differentiated SH-SY5Y cultures confirmed that BDNF subsequently released from this carrier retained its bioactivity. Accumulation of intravenously administered CAQK-targeted pSiNPs and their protein cargo in injured brain tissue was confirmed using a fluorescently tagged model protein in a CCI mouse model of TBI. When formulated with BDNF and administered systemically 2 hours post-injury, the CAQK-modified BDNF-loaded pSiNPs reduced brain lesion volumes by ~24% compared to treatment with PBS or free BDNF. This work demonstrates that ligand-targeted pSiNPs can be used to deliver a therapeutic protein cargo to injured brains after systemic administration, and that this treatment leads to phenotypic improvements in a TBI animal model.

The positive results seen in this study for treatment of TBI suggest that systemic and targeted delivery of BDNF using nanoparticles may also have potential in other central nervous system injuries. For example, BDNF is a promising therapeutic for stroke[92-95] and spinal cord injury.[17,18,96,97] Additionally, the progressive deterioration that occurs after TBI is caused by multiple disease pathways, such as ROS generation, inflammation, and vascular dysfunction.[4] It has been hypothesized that monotherapies are insufficient to address the multi-factor disease pathology of TBI and combination therapy may be a key to overcome the decades of failed TBI clinical trials.[98] Due to their versatile chemistry and tunable pore size, pSiNPs provide a promising platform technology for multiple therapeutic cargos in combination therapies that might better address the multi-factorial causes of TBI disease pathology.

## EXPERIMENTAL PROCEDURES

### Materials.

CAQK peptide and fluorescein-conjugated peptide FAM-CAQK were purchased from CPC Scientific, Inc. (San Jose, CA). Highly boron-doped p-type silicon wafers, 1.2 mΩ-cm resistivity, single-side polished on the (100) face, were obtained from Virginia Semiconductor (USA). Concentrated hydrofluoric acid (HF, 48% aqueous, ACS grade) was obtained from Fisher Scientific (USA). Succinimidyl valerate-polyethylene glycol-maleimide (SVA-PEG-MAL, MW 5 kDa) was purchased from Laysan Bio (Arab, AL). Absolute ethanol, methanol, and 3-(Ethoxydimethylsilyl)propyl-amine (APDMES) were obtained from Sigma-Aldrich (St. Louis, MO). BDNF was obtained from R&D Systems (USA).

### Synthesis of pSiNPs.

The preparation followed a published "perforated etch" procedure.[99] Single-crystalline highly doped p-type silicon wafers were anodically etched in an electrolyte consisting of hydrofluoric acid (48%) and ethanol in a 3:1 ratio by volume. CAUTION: HF is highly toxic and corrosive and contact with skin should be avoided. Procedures involving HF should always be carried out in a fume hood configured to handle HF and the operator should wear appropriate protective gloves, gown, and face shield. Etching was carried out in a Teflon etch cell using a platinum coil counter electrode. Prior to preparation of the porous silicon layers, the wafer surface was cleaned using a sacrificial etch consisting of electrochemical

anodization (60 sec, 46 mA/cm$^2$) in the HF electrolyte, followed by ethanol rinse, then dissolution of the resulting porous film with aqueous KOH (1 M). The wafer was then rinsed with water (1x) and ethanol (2x). An etching waveform consisting of a square wave of 200 cycles, in which a lower value of current density of 46 mA/cm$^2$ was applied for 1.2 s, followed by an upper value of current density of 365 mA/cm$^2$ applied for 0.363 s (Keithley 2651A Sourcemeter power supply). The multilayered porous nanostructure was removed from the crystalline silicon substrate by application of current pulse of 3.7 mA/cm$^2$ for 250 s in an electrolyte consisting of 1:29 (v:v) of 48% aqueous HF:absolute ethanol. The freestanding porous silicon sheets were placed in a sealed vial containing 1 mL of deionized water per mg of porous silicon and subjected to ultrasonic fracture in an ultrasonic bath (model 97043-960, VWR International) operating at a frequency of 35KHz and power of 48 Watts with a 1.9 L capacity overnight. The resulting ~130 nm-diameter nanoparticles were collected using centrifugation (15,000 rpm, 10 min, Eppendorf Centrifuge Model 5424R) and washed 3 times with ethanol and then isolated by centrifugation. Nanoparticles prepared in this manner are mesoporous, consisting of a crystalline silicon core skeleton coated with a surface layer of silicon dioxide.

1 mg of the pSiNPs resulting from the above procedure were washed once with DI water and then suspended in 1 mL of a solution consisting of recombinant human BDNF (200 μg/mL) dissolved in DI water. The nanoparticles were incubated under constant agitation at room temperature for ~18 hours. For the experiments involving the model protein lysozyme with conjugated Rhodamine B, the protein was loaded in a similar fashion. Protein mass loading was determined by measuring protein concentrations remaining in the supernatant after centrifugation by either BCA (lysozyme) or ELISA (BDNF; BDNF DuoSet ELISA, R&D Systems). The nanoparticles were washed once in DI water (via centrifugation/resuspension) to remove any unloaded protein from the solution, and then subsequently with 70% ethanol and finally with 100% ethanol. The loaded nanoparticles were aminated by incubation in an ethanol solution containing 12 μL/mL of APDMES for 3 hours under constant agitation. The nanoparticles were washed 3 times in 100% ethanol to remove any additional APDMES and incubated for 1 hour with 5 kDa SVA-PEG-MAL (500 μg in 1 mL ethanol) with constant agitation to achieve a PEGylated surface. After 3 more washes with 100% ethanol to remove any additional PEG, the nanoparticles were incubated with CAQK (100 μg/1 mg pSiNPs) overnight at room temperature. The nanoparticles were washed with 100% ethanol, 70% ethanol, and water and resuspended in water for characterization and use.

### Characterization of pSiNPs.

A Malvern Zetasizer Nano (Malvern Panalytical Ltd.) was used to determine the hydrodynamic diameter and zeta potential of the nanoparticles. A Thermo Scientific Nicolet 6700 FTIR instrument fitted with a Smart iTR diamond ATR fixture was used to determine the FTIR spectra of the nanoparticles. A Genesys 150 UV/VIS Spectrophotometer (Thermo Fisher Scientific, Inc.) was used to evaluate the absorbance of FAM-peptide and a NanoSight LM10-HSB/GFT14 (Malvern Panalytical Ltd.) was used to determine the concentration of pSiNPs to calculate the number of peptides conjugated per pSiNP. For degradation studies, 0.5 mg/mL of lysozyme-loaded pSiNPs surface modified with PEG and CAQK were incubated in PBS at 37 °C. At 0, 12, 24, and 48 hours, aliquots of degraded nanoparticles

were removed from the stock, pelleted, and resuspended into ethanol and loaded onto 42 μm formvar/carbon 400 mesh copper grids (Ted Pella, Inc.) and dried. The stock nanoparticles were similarly pelleted at each timepoint and resuspended in fresh PBS to ensure that degradation would not be stalled by the solubility of silicic acid in the supernatant.[29] TEM images were obtained on a JEOL 1400 plus electron microscope (JEOL USA, Inc.) operated at 80KeV and equipped with a Gatan Oneview camera (Gatan, Inc.).

### Measurement of Protein Release from pSiNPs.

0.5 mg/mL of lysozyme or BDNF-loaded pSiNPs and an equivalent concentration of control nanoparticles were incubated in PBS at 37 °C. For release assays, supernatant was collected every 24 hours for up to 4 days and evaluated for protein concentration by BCA or ELISA. The percent protein release was calculated from the total cumulative release over the experiment. Cumulative released BDNF was calculated to be 51 ± 1.3% of BDNF calculated during loading. Lysozyme activity was determined by a Micrococcus lysodeikticus cell assay as previously described with some modification.[60] Briefly, 0.5 mg/mL of lysozyme loaded pSiNP were incubated within a solution containing M. lysodeikticus cells. Lysozyme activity was evaluated by measuring the absorbance of the intact cells at 450 nm using a plate reader (Tecan) over 5 minutes.

### Bioactivity of BDNF in Retinoic Acid Differentiated SH-SY5Y Cultures.

SH-SY5Y cells (ATCC) were plated at 32,000 cells/cm$^2$ in 96 well plates or at 16,000 cells/cm$^2$ on cover glasses coated sequentially in 0.05 mg/mL poly-D-lysine overnight and 0.05 mg/mL rat tail collagen 1 for 2 hours at 37°C. Cells were cultured in Minimum Essential Medium (MEM) supplemented with 10% fetal bovine serum (FBS) and 1% penicillin-streptomycin for 24 hours before beginning the differentiation protocol. 10 μM retinoic acid in full media was introduced to the cells through a media change starting 24 hours after plating and exchanged every 48 hours. Cells were differentiated for 5 days to induce TrkB expression before beginning BDNF bioactivity studies.[68,69] For viability studies, doses ranging from 600 ng/mL (equivalent to 4.5 μg/mL pSiNP) to 0 ng/mL of free BDNF, pSiNP-BDNF surface modified with PEG, or pSiNP vehicles surface modified with PEG in serum-free MEM were introduced to the retinoic acid treated SH-SY5Y cells through a media change after washing the cells twice in serum-free MEM. Control wells representing 100% cell viability received full media with 10 μM retinoic acid. Cells were treated for 2 days and cell viability was evaluated with a CellTiter-Glo® Assay (Promega). For morphology studies, cells were cultured with treatments at 300 ng/mL for 3 days before being fixed and stained with anti-NF200 (Sigma), FITC-phalloidin (Millipore Sigma), and Hoechst with standard protocols. Fluorescent images were obtained on a Nikon Eclipse Ti2 (Nikon Instruments Inc.) of quadruplicate cover glasses.

### Animal Injury Model.

All animal experiments were approved by the University of California, San Diego Institutional Animal Care and Use Committee (IACUC). A CCI model of TBI in mice was used for this study. 8-week-old C57BL/6J female mice (Jackson Labs) were placed in a stereotaxic frame under 2.5% isoflurane anesthesia and a 5 mm diameter craniotomy was performed over the right cortex, adjacent to the midline of the skull and midway between

lambda and bregma. The right cortex was injured at a 2 mm depth with a 2 mm diameter stainless steel piston tip at a rate of 3 m/s using an ImpactOne (Leica Biosystems).

### Protein Delivery from pSiNPs Targeting the Injured Brain in vivo.

Lysozyme-loaded pSiNPs surface modified with PEG and CAQK were injected *via* the tail-vein 2 hours after CCI (n=3) with control groups receiving pSiNP-Lysozyme-PEG-CAQK without injury or receiving an injury with a control PBS injection. Mice were perfused and brains were harvested 2 hours after injection. Time gated imaging was performed with an iSTAR 334T CCD camera (Andor Technology Ltd.) fitted with a Nikon AF micro lens (Nikko 105 mm) with laser excitation at 410 nm and a long-pass filter at 460 nm to quantify pSiNP localization. Brains were equilibrated in 30% w/v sucrose overnight and frozen in OCT (Tissue-Tek). Coronal sections were taken from the whole brain and counterstained with Hoechst to image the presence of Rhodamine B-tagged lysozyme being released from the pSiNPs which were tagged by FAM-labeled CAQK.

For BDNF treatments, 28 mice (n=7) were divided into 4 groups; PBS treated control, pSiNP-BDNF treatment surface modified with PEG-CAQK (13 μg BDNF equivalent, 100 μg pSiNPs), free BDNF treatment (20 μg), and a vehicle-only treatment (100 μg unloaded pSiNPs surface modified with PEG-CAQK) (Figure 4a).[33] 2 hours after CCI, treatments were administered intravenously through a tail-vein injection. Brains were collected 72 hours post-injury after perfusion with 10% formalin and frozen in OCT for tissue processing.

### Lesion Volume Analysis and Histology.

10-μm thick coronal sections were taken every 0.5 mm from coordinates −4 mm to 1 mm from bregma for lesion analysis and processed with H&E staining to clearly visualize the lesion area with brightfield microscopy. Images of each section were blindly analyzed for lesion size by measuring the outlined lesion area using ImageJ software. Lesion volume was calculated with the trapezoidal rule. Sections taken from the center of each injury were Nissl stained using conventional protocols. Slides were imaged automatically using a Zeiss Axio Scan.Z1 and imaged with a color camera using a Nikon Eclipse Ti2 (Nikon Instruments Inc.).

### Statistical Analysis.

Statistical analysis was performed on GraphPad Prism 8 software (9.1.2). In Figure 3b, cell viability was analyzed with a two-way ANOVA and Dunnett's post hoc test conducted with $p<0.05$. In Figure 4b, lesion volume was analyzed with a one-way ANOVA with Dunnett's post hoc test conducted with $p<0.05$.

## Supplementary Material

Refer to Web version on PubMed Central for supplementary material.

## ACKNOWLEDGEMENTS

This work was supported by National Institutes of Health (NIH) Director's New Innovator Award (Number DP2 NS111507), by the National Science Foundation (NSF) through the University of California, San Diego Materials Research Science and Engineering Center (UCSD MRSEC, Award number DMR-2011924), and by the NIH (R01 AI132413). This work was performed in part at the San Diego Nanotechnology Infrastructure (SDNI) of the University of California, San Diego, a member of the National Nanotechnology Coordinated Infrastructure, which is supported by the NSF (Grant ECCS-1542148). The authors acknowledge the use of facilities and instrumentation supported by NSF through the University of California, San Diego Materials Research Science and Engineering Center (Award number DMR-2011924). The authors also would like to thank the University of California, San Diego - Cellular and Molecular Medicine Electron Microscopy Core (UCSD-CMM-EM Core, RRID:SCR_022039) for equipment access and technical assistance. The UCSD-CMM-EM Core is supported in part by the NIH (Award number S10OD023527).

## ABBREVIATIONS

| | |
|---|---|
| **AAV2** | Adeno-associated Virus Vector |
| **APDMES** | 3-(Ethoxydimethylsilyl)propyl-amine |
| **BBB** | Blood-brain Barrier |
| **BDNF** | Brain-derived Neurotrophic Factor |
| **CCI** | Controlled Cortical Impact |
| **DLS** | Dynamic Light Scattering |
| **ECM** | Extracellular Matrix |
| **FBS** | Fetal Bovine Serum |
| **FTIR** | Fourier-transform Infrared Spectroscopy |
| **HF** | Hydrofluoric Acid |
| **IACUC** | Institutional Animal Care and Use Committee |
| **MEM** | Minimum Essential Media |
| **NGF** | Nerve Growth Factor |
| **PBS** | Phosphate-buffered Saline |
| **PEG** | Polyethylene Glycol |
| **PLGA** | Poly(lactic-co-glycolic Acid) |
| **pSiNP** | Porous Silicon Nanoparticle |
| **ROS** | Reactive Oxygen Species |
| **SVA-PEG-MAL** | Succinimidyl Valerate-Polyethylene glycol-Maleimide |
| **TBI** | Traumatic Brain Injury |
| **TEM** | Transmission Electron Microscopy |

**TrkB** Tropomyosin Receptor Kinase B

## REFERENCES


(1). Surveillance Report of Traumatic Brain Injury-Related Emergency Department Visits, Hospitalizations, and Deaths

(2). Dean PJA; Sterr A Long-Term Effects of Mild Traumatic Brain Injury on Cognitive Performance. Front. Hum. Neurosci 2013, 7. 10.3389/fnhum.2013.00030.

(3). Vanderploeg RD; Curtiss G; Belanger HG Long-Term Neuropsychological Outcomes Following Mild Traumatic Brain Injury. J. Int. Neuropsychol. Soc 2005, 11 (3), 228–236. 10.1017/S1355617705050289. [PubMed: 15892899]

(4). Werner C; Engelhard K Pathophysiology of Traumatic Brain Injury. Br. J. Anaesth 2007, 99 (1), 4–9. 10.1093/bja/aem131. [PubMed: 17573392]

(5). Nagahara AH; Tuszynski MH Potential Therapeutic Uses of BDNF in Neurological and Psychiatric Disorders. Nat. Rev. Drug Discov 2011, 10 (3), 209–219. 10.1038/nrd3366. [PubMed: 21358740]

(6). Huang EJ; Reichardt LF Neurotrophins: Roles in Neuronal Development and Function. Annu. Rev. Neurosci 2001, 24, 677–736. 10.1146/annurev.neuro.24.1.677. [PubMed: 11520916]

(7). Wurzelmann M; Romeika J; Sun D Therapeutic Potential of Brain-Derived Neurotrophic Factor (BDNF) and a Small Molecular Mimics of BDNF for Traumatic Brain Injury. Neural Regen. Res 2017, 12 (1), 7–12. 10.4103/1673-5374.198964. [PubMed: 28250730]

(8). Klein R; Martin-Zanca D; Acid MB; Parada LF Expression of the Tyrosine Kinase Receptor Gene TrkB Is Confined to the Murine Embryonic and Adult Nervous System. 10.

(9). Huang EJ; Reichardt LF Trk Receptors: Roles in Neuronal Signal Transduction. Annu. Rev. Biochem 2003, 72 (1), 609–642. 10.1146/annurev.biochem.72.121801.161629. [PubMed: 12676795]

(10). Kaplan DR; Miller FD Neurotrophin Signal Transduction in the Nervous System. Curr. Opin. Neurobiol 2000, 10 (3), 381–391. 10.1016/s0959-4388(00)00092-1. [PubMed: 10851172]

(11). Xiong L-L; Hu Y; Zhang P; Zhang Z; Li L-H; Gao G-D; Zhou X-F; Wang T-H Neural Stem Cell Transplantation Promotes Functional Recovery from Traumatic Brain Injury via Brain Derived Neurotrophic Factor-Mediated Neuroplasticity. Mol. Neurobiol 2018, 55 (3), 2696–2711. 10.1007/s12035-017-0551-1. [PubMed: 28421542]

(12). Lu P; Jones LL; Snyder EY; Tuszynski MH Neural Stem Cells Constitutively Secrete Neurotrophic Factors and Promote Extensive Host Axonal Growth after Spinal Cord Injury. Exp. Neurol 2003, 181 (2), 115–129. 10.1016/S0014-4886(03)00037-2. [PubMed: 12781986]

(13). Blurton-Jones M; Kitazawa M; Martinez-Coria H; Castello NA; Muller F-J; Loring JF; Yamasaki TR; Poon WW; Green KN; LaFerla FM Neural Stem Cells Improve Cognition via BDNF in a Transgenic Model of Alzheimer Disease. Proc. Natl. Acad. Sci 2009, 106 (32), 13594–13599. 10.1073/pnas.0901402106. [PubMed: 19633196]

(14). Fink KD; Deng P; Torrest A; Stewart H; Pollock K; Gruenloh W; Annett G; Tempkin T; Wheelock V; Nolta JA Developing Stem Cell Therapies for Juvenile and Adult-Onset Huntington's Disease. Regen. Med 2015, 10 (5), 623–646. 10.2217/rme.15.25. [PubMed: 26237705]

(15). Frim DM; Uhler TA; Galpern WR; Beal MF; Breakefield XO; Isacson O Implanted Fibroblasts Genetically Engineered to Produce Brain-Derived Neurotrophic Factor Prevent 1-Methyl-4-Phenylpyridinium Toxicity to Dopaminergic Neurons in the Rat. Proc. Natl. Acad. Sci. U. S. A 1994, 91 (11), 5104–5108. [PubMed: 8197193]

(16). Pollock K; Dahlenburg H; Nelson H; Fink KD; Cary W; Hendrix K; Annett G; Torrest A; Deng P; Gutierrez J; et al. Human Mesenchymal Stem Cells Genetically Engineered to Overexpress Brain-Derived Neurotrophic Factor Improve Outcomes in Huntington's Disease Mouse Models. Mol. Ther 2016, 24 (5), 965–977. 10.1038/mt.2016.12. [PubMed: 26765769]

(17). Tobias CA; Shumsky JS; Shibata M; Tuszynski MH; Fischer I; Tessler A; Murray M Delayed Grafting of BDNF and NT-3 Producing Fibroblasts into the Injured Spinal Cord Stimulates Sprouting, Partially Rescues Axotomized Red Nucleus Neurons from Loss and

Atrophy, and Provides Limited Regeneration. Exp. Neurol 2003, 184 (1), 97–113. 10.1016/S0014-4886(03)00394-7. [PubMed: 14637084]

(18). Blesch A; Tuszynski MH Transient Growth Factor Delivery Sustains Regenerated Axons after Spinal Cord Injury. J. Neurosci 2007, 27 (39), 10535–10545. 10.1523/JNEUROSCI.1903-07.2007. [PubMed: 17898225]

(19). Nagahara AH; Merrill DA; Coppola G; Tsukada S; Schroeder BE; Shaked GM; Wang L; Blesch A; Kim A; Conner JM; et al. Neuroprotective Effects of Brain-Derived Neurotrophic Factor in Rodent and Primate Models of Alzheimer's Disease. Nat. Med 2009, 15 (3), 331–337. 10.1038/nm.1912. [PubMed: 19198615]

(20). Menon PK; Muresanu DF; Sharma A; Mossler H; Sharma HS Cerebrolysin, a Mixture of Neurotrophic Factors Induces Marked Neuroprotection in Spinal Cord Injury Following Intoxication of Engineered Nanoparticles from Metals. CNS Neurol. Disord. - Drug Targets 2012, 11 (1), 40–49. 10.2174/187152712799960781. [PubMed: 22229324]

(21). Ghaffarpasand F; Torabi S; Rasti A; Niakan MH; Aghabaklou S; Pakzad F; Beheshtian MS; Tabrizi R Effects of Cerebrolysin on Functional Outcome of Patients with Traumatic Brain Injury: A Systematic Review and Meta-Analysis. Neuropsychiatr. Dis. Treat 2018, 15, 127–135. 10.2147/NDT.S186865. [PubMed: 30643411]

(22). First-in-Human Clinical Trial to Assess Gene Therapy for Alzheimer's Disease. https://ucsdnews.ucsd.edu/pressrelease/first-in-human-clinical-trial-to-assess-gene-therapy-for-alzheimers-disease.

(23). Price R; Milne S; Sharkey J; Matsuoka N Advances in Small Molecules Promoting Neurotrophic Function. Pharmacol. Ther 2007, 115 (2), 292–306. 10.1016/j.pharmthera.2007.03.005. [PubMed: 17599430]

(24). Géral C; Angelova A; Lesieur S From Molecular to Nanotechnology Strategies for Delivery of Neurotrophins: Emphasis on Brain-Derived Neurotrophic Factor (BDNF). Pharmaceutics 2013, 5 (1), 127–167. 10.3390/pharmaceutics5010127. [PubMed: 24300402]

(25). Emerich DF; Thanos CG The Pinpoint Promise of Nanoparticle-Based Drug Delivery and Molecular Diagnosis. Biomol. Eng 2006, 23 (4), 171–184. 10.1016/j.bioeng.2006.05.026. [PubMed: 16843058]

(26). Lampe KJ; Kern DS; Mahoney MJ; Bjugstad KB The Administration of BDNF and GDNF to the Brain via PLGA Microparticles Patterned within a Degradable PEG-Based Hydrogel: Protein Distribution and the Glial Response. J. Biomed. Mater. Res. A 2011, 96A (3), 595–607. 10.1002/jbm.a.33011.

(27). Bertram JP; Rauch MF; Chang K; Lavik EB Using Polymer Chemistry to Modulate the Delivery of Neurotrophic Factors from Degradable Microspheres: Delivery of BDNF. Pharm. Res 2010, 27 (1), 82–91. 10.1007/s11095-009-0009-x. [PubMed: 19921405]

(28). Wang Y; Wei YT; Zu ZH; Ju RK; Guo MY; Wang XM; Xu QY; Cui FZ Combination of Hyaluronic Acid Hydrogel Scaffold and PLGA Microspheres for Supporting Survival of Neural Stem Cells. Pharm. Res 2011, 28 (6), 1406. 10.1007/s11095-011-0452-3. [PubMed: 21537876]

(29). Park J-H; Gu L; von Maltzahn G; Ruoslahti E; Bhatia SN; Sailor MJ Biodegradable Luminescent Porous Silicon Nanoparticles for in Vivo Applications. Nat. Mater 2009, 8 (4), 331–336. 10.1038/nmat2398. [PubMed: 19234444]

(30). Foraker AB; Walczak RJ; Cohen MH; Boiarski TA; Grove CF; Swaan PW Microfabricated Porous Silicon Particles Enhance Paracellular Delivery of Insulin Across Intestinal Caco-2 Cell Monolayers. 7.

(31). Kang J; Joo J; Kwon EJ; Skalak M; Hussain S; She Z-G; Ruoslahti E; Bhatia SN; Sailor MJ Self-Sealing Porous Silicon-Calcium Silicate Core–Shell Nanoparticles for Targeted SiRNA Delivery to the Injured Brain. Adv. Mater 2016, 28 (36), 7962–7969. 10.1002/adma.201600634. [PubMed: 27383373]

(32). Kim D; Zuidema JM; Kang J; Pan Y; Wu L; Warther D; Arkles B; Sailor MJ Facile Surface Modification of Hydroxylated Silicon Nanostructures Using Heterocyclic Silanes. J. Am. Chem. Soc 2016, 138 (46), 15106–15109. 10.1021/jacs.6b08614. [PubMed: 27933884]

(33). Mann AP; Scodeller P; Hussain S; Joo J; Kwon E; Braun GB; Mölder T; She Z-G; Kotamraju VR; Ranscht B; et al. A Peptide for Targeted, Systemic Delivery of Imaging and Therapeutic

Compounds into Acute Brain Injuries. Nat. Commun 2016, 7 (1), 11980. 10.1038/ncomms11980. [PubMed: 27351915]

(34). Zuidema JM; Kumeria T; Kim D; Kang J; Wang J; Hollett G; Zhang X; Roberts DS; Chan N; Dowling C; Blanco-Suarez E; et al. Oriented Nanofibrous Polymer Scaffolds Containing Protein-Loaded Porous Silicon Generated by Spray Nebulization. Adv. Mater 2018, 30 (12), 1706785. 10.1002/adma.201706785.

(35). Kwon EJ; Skalak M; Bertucci A; Braun G; Ricci F; Ruoslahti E; Sailor MJ; Bhatia SN Porous Silicon Nanoparticle Delivery of Tandem Peptide Anti-Infectives for the Treatment of Pseudomonas Aeruginosa Lung Infections. Adv. Mater 2017, 29 (35), 1701527. 10.1002/adma.201701527.

(36). Li W; Liu Z; Fontana F; Ding Y; Liu D; Hirvonen JT; Santos HA Tailoring Porous Silicon for Biomedical Applications: From Drug Delivery to Cancer Immunotherapy. Adv. Mater 2018, 30 (24), 1703740. 10.1002/adma.201703740.

(37). Bertucci A; Kim K-H; Kang J; Zuidema JM; Lee SH; Kwon EJ; Kim D; Howell SB; Ricci F; Ruoslahti E; et al. Tumor-Targeting, MicroRNA-Silencing Porous Silicon Nanoparticles for Ovarian Cancer Therapy. ACS Appl. Mater. Interfaces 2019, 11 (27), 23926–23937. 10.1021/acsami.9b07980. [PubMed: 31251556]

(38). Zuidema JM; Dumont CM; Wang J; Batchelor WM; Lu Y-S; Kang J; Bertucci A; Ziebarth NM; Shea LD; Sailor MJ Porous Silicon Nanoparticles Embedded in Poly(Lactic-Co-Glycolic Acid) Nanofiber Scaffolds Deliver Neurotrophic Payloads to Enhance Neuronal Growth. Adv. Funct. Mater 2020, 30 (25), 2002560. 10.1002/adfm.202002560. [PubMed: 32982626]

(39). Kumeria T; Wang J; Kim B; Park J-H; Zuidema JM; Klempner M; Cavacini L; Wang Y; Sailor MJ Enteric Polymer-Coated Porous Silicon Nanoparticles for Site-Specific Oral Delivery of IgA Antibody. ACS Biomater. Sci. Eng 2020. 10.1021/acsbiomaterials.0c01313.

(40). Zilony-Hanin N; Rosenberg M; Richman M; Yehuda R; Schori H; Motiei M; Rahimipour S; Groisman A; Segal E; Shefi O Neuroprotective Effect of Nerve Growth Factor Loaded in Porous Silicon Nanostructures in an Alzheimer's Disease Model and Potential Delivery to the Brain. Small 2019, 15 (45), 1904203. 10.1002/smll.201904203.

(41). Rosenberg M; Zilony N; Shefi O; Segal E Designing Porous Silicon Films as Carriers of Nerve Growth Factor. JoVE J. Vis. Exp 2019, No. 143, e58982. 10.3791/58982.

(42). Wu C-C; Hu Y; Miller M; Aroian RV; Sailor MJ Protection and Delivery of Anthelmintic Protein Cry5B to Nematodes Using Mesoporous Silicon Particles. ACS Nano 2015, 9 (6), 6158–6167. 10.1021/acsnano.5b01426. [PubMed: 25950754]

(43). Henstock JR; Canham LT; Anderson SI Silicon: The Evolution of Its Use in Biomaterials. Acta Biomater. 2015, 11, 17–26. 10.1016/j.actbio.2014.09.025. [PubMed: 25246311]

(44). Andrew JS; Anglin EJ; Wu EC; Chen MY; Cheng L; Freeman WR; Sailor MJ Sustained Release of a Monoclonal Antibody from Electrochemically Prepared Mesoporous Silicon Oxide. Adv. Funct. Mater 2010, 20 (23), 4168–4174. 10.1002/adfm.201000907. [PubMed: 21274422]

(45). Wang J; Kumeria T; Bezem MT; Wang J; Sailor MJ Self-Reporting Photoluminescent Porous Silicon Microparticles for Drug Delivery. ACS Appl. Mater. Interfaces 2018, 10 (4), 3200–3209. 10.1021/acsami.7b09071. [PubMed: 29278488]

(46). Zilony-Hanin N; Rosenberg M; Richman M; Yehuda R; Schori H; Motiei M; Rahimipour S; Groisman A; Segal E; Shefi O Neuroprotective Effect of Nerve Growth Factor Loaded in Porous Silicon Nanostructures in an Alzheimer's Disease Model and Potential Delivery to the Brain. Small 2019, 15 (45), 1904203. 10.1002/smll.201904203.

(47). Fong R; Konakondla S; Schirmer CM; Lacroix M Surgical Interventions for Severe Traumatic Brain Injury. J. Emerg. Crit. Care Med 2017, 1 (10). 10.21037/jeccm.2017.09.03.

(48). Kwon EJ; Skalak M; Lo Bu R; Bhatia SN Neuron-Targeted Nanoparticle for SiRNA Delivery to Traumatic Brain Injuries. ACS Nano 2016, 10 (8), 7926–7933. 10.1021/acsnano.6b03858. [PubMed: 27429164]

(49). Boyd BJ; Galle A; Daglas M; Rosenfeld JV; Medcalf R Traumatic Brain Injury Opens Blood–Brain Barrier to Stealth Liposomes via an Enhanced Permeability and Retention (EPR)-like Effect. J. Drug Target 2015, 23 (9), 847–853. 10.3109/1061186X.2015.1034280. [PubMed: 26079716]

(50). Kudryashev JA; Waggoner LE; Leng HT; Mininni NH; Kwon EJ An Activity-Based Nanosensor for Traumatic Brain Injury. ACS Sens. 2020, 5 (3), 686–692. 10.1021/acssensors.9b01812. [PubMed: 32100994]

(51). Bharadwaj VN; Lifshitz J; Adelson PD; Kodibagkar VD; Stabenfeldt SE Temporal Assessment of Nanoparticle Accumulation after Experimental Brain Injury: Effect of Particle Size. Sci. Rep 2016, 6 (1), 29988. 10.1038/srep29988. [PubMed: 27444615]

(52). Cunningham TL; Cartagena CM; Lu X-CM; Konopko M; Dave JR; Tortella FC; Shear DA Correlations between Blood–Brain Barrier Disruption and Neuroinflammation in an Experimental Model of Penetrating Ballistic-Like Brain Injury. J. Neurotrauma 2014, 31 (5), 505–514. 10.1089/neu.2013.2965. [PubMed: 24138024]

(53). Wetter LR; Deutsch HF Immunological Studies on Egg White Proteins Iv. Immunochemical and Physical Studies of Lysozyme. J. Biol. Chem 1951, 192 (1), 237–242. [PubMed: 14917670]

(54). Hempstead BL Brain-Derived Neurotrophic Factor: Three Ligands, Many Actions. Trans. Am. Clin. Climatol. Assoc 2015, 126, 9. [PubMed: 26330656]

(55). Gole A; Thakar J; Sastry M Protein Diffusion into Thermally Evaporated Lipid Films: Role of Protein Charge/Mass Ratio. Colloids Surf. B Biointerfaces 2003, 28 (2–3), 209–214. 10.1016/S0927-7765(02)00141-8.

(56). Harris JM; Martin NE; Modi M Pegylation. Clin. Pharmacokinet 2001, 40 (7), 539–551. 10.2165/00003088-200140070-00005. [PubMed: 11510630]

(57). Harris JM; Chess RB Effect of Pegylation on Pharmaceuticals. Nat. Rev. Drug Discov 2003, 2 (3), 214–221. 10.1038/nrd1033. [PubMed: 12612647]

(58). Chieng B; Ibrahim N; Yunus W; Hussein M Poly(Lactic Acid)/Poly(Ethylene Glycol) Polymer Nanocomposites: Effects of Graphene Nanoplatelets. Polymers 2013, 6 (1), 93–104. 10.3390/polym6010093.

(59). Jokerst JV; Lobovkina T; Zare RN; Gambhir SS Nanoparticle PEGylation for Imaging and Therapy. Nanomed. 2011, 6 (4), 715–728. 10.2217/nnm.11.19.

(60). Jiang Z-L; Huang G-X Resonance Scattering Spectra of Micrococcus Lysodeikticus and Its Application to Assay of Lysozyme Activity. Clin. Chim. Acta 2007, 376 (1), 136–141. 10.1016/j.cca.2006.08.005. [PubMed: 16979609]

(61). Shen J; Xu R; Mai J; Kim H-C; Guo X; Qin G; Yang Y; Wolfram J; Mu C; Xia X; et al. High Capacity Nanoporous Silicon Carrier for Systemic Delivery of Gene Silencing Therapeutics. ACS Nano 2013, 7 (11), 9867–9880. 10.1021/nn4035316. [PubMed: 24131405]

(62). Joo J; Kwon EJ; Kang J; Skalak M; Anglin EJ; Mann AP; Ruoslahti E; Bhatia SN; Sailor MJ Porous Silicon–Graphene Oxide Core–Shell Nanoparticles for Targeted Delivery of SiRNA to the Injured Brain. Nanoscale Horiz. 2016, 1 (5), 407–414. 10.1039/C6NH00082G. [PubMed: 29732165]

(63). Popplewell JF; King SJ; Day JP; Ackrill P; Fifield LK; Cresswell RG; di Tada ML; Liu K Kinetics of Uptake and Elimination of Silicic Acid by a Human Subject: A Novel Application of 32Si and Accelerator Mass Spectrometry. J. Inorg. Biochem 1998, 69 (3), 177–180. 10.1016/S0162-0134(97)10016-2. [PubMed: 9629677]

(64). Jin Y; Kim D; Roh H; Kim S; Hussain S; Kang J; Pack C-G; Kim JK; Myung S-J; Ruoslahti E; et al. Tracking the Fate of Porous Silicon Nanoparticles Delivering a Peptide Payload by Intrinsic Photoluminescence Lifetime. Adv. Mater 2018, 30 (35), 1802878. 10.1002/adma.201802878.

(65). Tzur-Balter A; Shatsberg Z; Beckerman M; Segal E; Artzi N Mechanism of Erosion of Nanostructured Porous Silicon Drug Carriers in Neoplastic Tissues. Nat. Commun 2015, 6 (1), 6208. 10.1038/ncomms7208. [PubMed: 25670235]

(66). Xiong Y; Mahmood A; Chopp M Animal Models of Traumatic Brain Injury. Nat. Rev. Neurosci 2013, 14 (2), 128–142. 10.1038/nrn3407. [PubMed: 23329160]

(67). Joo J; Liu X; Kotamraju VR; Ruoslahti E; Nam Y; Sailor MJ Gated Luminescence Imaging of Silicon Nanoparticles. ACS Nano 2015, 9 (6), 6233–6241. 10.1021/acsnano.5b01594. [PubMed: 26034817]

(68). Kaplan DR; Matsumoto K; Lucarelli E; Thielet CJ Induction of TrkB by Retinoic Acid Mediates Biologic Responsiveness to BDNF and Differentiation of Human Neuroblastoma Cells. Neuron 1993, 11 (2), 321–331. 10.1016/0896-6273(93)90187-V. [PubMed: 8394722]

(69). Encinas M; Iglesias M; Liu Y; Wang H; Muhaisen A; Ceña V; Gallego C; Comella JX Sequential Treatment of SH-SY5Y Cells with Retinoic Acid and Brain-Derived Neurotrophic Factor Gives Rise to Fully Differentiated, Neurotrophic Factor-Dependent, Human Neuron-Like Cells. J. Neurochem 2000, 75 (3), 991–1003. 10.1046/j.1471-4159.2000.0750991.x. [PubMed: 10936180]

(70). Dedoni S; Olianas MC; Ingianni A; Onali P Type I Interferons Impair BDNF-Induced Cell Signaling and Neurotrophic Activity in Differentiated Human SH-SY5Y Neuroblastoma Cells and Mouse Primary Cortical Neurons. J. Neurochem 2012, 122 (1), 58–71. 10.1111/j.1471-4159.2012.07766.x. [PubMed: 22533963]

(71). Encinas M; Iglesias M; Llecha N; Comella JX Extracellular-Regulated Kinases and Phosphatidylinositol 3-Kinase Are Involved in Brain-Derived Neurotrophic Factor-Mediated Survival and Neuritogenesis of the Neuroblastoma Cell Line SH-SY5Y. J. Neurochem 1999, 73 (4), 1409–1421. 10.1046/j.1471-4159.1999.0731409.x. [PubMed: 10501184]

(72). Kim H-J; Lee J-H; Kim S-H Therapeutic Effects of Human Mesenchymal Stem Cells on Traumatic Brain Injury in Rats: Secretion of Neurotrophic Factors and Inhibition of Apoptosis. J. Neurotrauma 2009, 27 (1), 131–138. 10.1089/neu.2008.0818.

(73). Ma H; Yu B; Kong L; Zhang Y; Shi Y Neural Stem Cells Over-Expressing Brain-Derived Neurotrophic Factor (BDNF) Stimulate Synaptic Protein Expression and Promote Functional Recovery Following Transplantation in Rat Model of Traumatic Brain Injury. Neurochem. Res 2012, 37 (1), 69–83. 10.1007/s11064-011-0584-1. [PubMed: 21901549]

(74). Wang Z; Yao W; Deng Q; Zhang X; Zhang J Protective Effects of BDNF Overexpression Bone Marrow Stromal Cell Transplantation in Rat Models of Traumatic Brain Injury. J. Mol. Neurosci 2013, 49 (2), 409–416. 10.1007/s12031-012-9908-0. [PubMed: 23143881]

(75). Sakane T; Pardridge WM Carboxyl-Directed Pegylation of Brain-Derived Neurotrophic Factor Markedly Reduces Systemic Clearance with Minimal Loss of Biologic Activity. Pharm. Res 1997, 14 (8), 1085–1091. 10.1023/A:1012117815460. [PubMed: 9279893]

(76). Poduslo JF; Curran GL Permeability at the Blood-Brain and Blood-Nerve Barriers of the Neurotrophic Factors: NGF, CNTF, NT-3, BDNF. Mol. Brain Res 1996, 36 (2), 280–286. 10.1016/0169-328X(95)00250-V. [PubMed: 8965648]

(77). Fukumitsu H; Ohtsuka M; Murai R; Nakamura H; Itoh K; Furukawa S Brain-Derived Neurotrophic Factor Participates in Determination of Neuronal Laminar Fate in the Developing Mouse Cerebral Cortex. J. Neurosci 2006, 26 (51), 13218–13230. 10.1523/JNEUROSCI.4251-06.2006. [PubMed: 17182772]

(78). Khalin I; Alyautdin R; Wong TW; Gnanou J; Kocherga G; Kreuter J Brain-Derived Neurotrophic Factor Delivered to the Brain Using Poly (Lactide-Co-Glycolide) Nanoparticles Improves Neurological and Cognitive Outcome in Mice with Traumatic Brain Injury. Drug Deliv. 2016, 23 (9), 3520–3528. 10.1080/10717544.2016.1199609. [PubMed: 27278330]

(79). Turtzo LC; Budde MD; Gold EM; Lewis BK; Janes L; Yarnell A; Grunberg NE; Watson W; Frank JA The Evolution of Traumatic Brain Injury in a Rat Focal Contusion Model. NMR Biomed. 2013, 26 (4), 468–479. 10.1002/nbm.2886. [PubMed: 23225324]

(80). Gennarelli TA; Spielman GM; Langfitt TW; Gildenberg PL; Harrington T; Jane JA; Marshall LF; Miller JD; Pitts LH Influence of the Type of Intracranial Lesion on Outcome from Severe Head Injury: A Multicenter Study Using a New Classification System. J. Neurosurg 1982, 56 (1), 26–32. 10.3171/jns.1982.56.1.0026. [PubMed: 7054419]

(81). Kenne E; Erlandsson A; Lindbom L; Hillered L; Clausen F Neutrophil Depletion Reduces Edema Formation and Tissue Loss Following Traumatic Brain Injury in Mice. J. Neuroinflammation 2012, 9 (1), 17. 10.1186/1742-2094-9-17. [PubMed: 22269349]

(82). Zhou H; Chen L; Gao X; Luo B; Chen J Moderate Traumatic Brain Injury Triggers Rapid Necrotic Death of Immature Neurons in the Hippocampus. J. Neuropathol. Exp. Neurol 2012, 71 (4), 348–359. 10.1097/NEN.0b013e31824ea078. [PubMed: 22437344]

(83). Hall ED; Sullivan PG; Gibson TR; Pavel KM; Thompson BM; Scheff SW Spatial and Temporal Characteristics of Neurodegeneration after Controlled Cortical Impact in Mice: More than a Focal Brain Injury. J. Neurotrauma 2005, 22 (2), 252–265. 10.1089/neu.2005.22.252. [PubMed: 15716631]

(84). Villapol S; Yaszemski AK; Logan TT; Sánchez-Lemus E; Saavedra JM; Symes AJ Candesartan, an Angiotensin II AT 1 -Receptor Blocker and PPAR-γ Agonist, Reduces

Lesion Volume and Improves Motor and Memory Function After Traumatic Brain Injury in Mice. Neuropsychopharmacology 2012, 37 (13), 2817–2829. 10.1038/npp.2012.152. [PubMed: 22892395]

(85). Wu Y; Wang J; Shi Y; Pu H; Leak RK; Liou AKF; Badylak SF; Liu Z; Zhang J; Chen J; et al. Implantation of Brain-Derived Extracellular Matrix Enhances Neurological Recovery after Traumatic Brain Injury. Cell Transplant. 2017, 26 (7), 1224–1234. 10.1177/0963689717714090. [PubMed: 28933217]

(86). Gu Y; Zhang J; Zhao Y; Su Y; Zhang Y Potassium Aspartate Attenuates Brain Injury Induced by Controlled Cortical Impact in Rats Through Increasing Adenosine Triphosphate (ATP) Levels, Na+/K+-ATPase Activity and Reducing Brain Edema. Med. Sci. Monit 2016, 22, 4894–4901. 10.12659/MSM.898185. [PubMed: 27959885]

(87). Park H-J; Machado AG; Cooperrider J; Truong H; Johnson M; Krishna V; Chen Z; Gale JT Semi-Automated Method for Estimating Lesion Volumes. J. Neurosci. Methods 2013, 213 (1), 76–83. 10.1016/j.jneumeth.2012.12.010. [PubMed: 23261655]

(88). Weber JT Altered Calcium Signaling Following Traumatic Brain Injury. Front. Pharmacol 2012, 3. 10.3389/fphar.2012.00060.

(89). Kabu S; Jaffer H; Petro M; Dudzinski D; Stewart D; Courtney A; Courtney M; Labhasetwar V Blast-Associated Shock Waves Result in Increased Brain Vascular Leakage and Elevated ROS Levels in a Rat Model of Traumatic Brain Injury. PLOS ONE 2015, 10 (5), e0127971. 10.1371/journal.pone.0127971. [PubMed: 26024446]

(90). Xie B-S; Wang Y-Q; Lin Y; Mao Q; Feng J-F; Gao G-Y; Jiang J-Y Inhibition of Ferroptosis Attenuates Tissue Damage and Improves Long-Term Outcomes after Traumatic Brain Injury in Mice. CNS Neurosci. Ther 2019, 25 (4), 465–475. 10.1111/cns.13069. [PubMed: 30264934]

(91). Oyesiku NM; Evans C-O; Houston S; Darrell RS; Smith JS; Fulop ZL; Dixon CE; Stein DG Regional Changes in the Expression of Neurotrophic Factors and Their Receptors Following Acute Traumatic Brain Injury in the Adult Rat Brain. Brain Res. 1999, 833 (2), 161–172. 10.1016/S0006-8993(99)01501-2. [PubMed: 10375691]

(92). van Velthoven CTJ; Sheldon RA; Kavelaars A; Derugin N; Vexler ZS; Willemen HLDM; Maas M; Heijnen CJ; Ferriero DM Mesenchymal Stem Cell Transplantation Attenuates Brain Injury After Neonatal Stroke. Stroke 2013, 44 (5), 1426–1432. 10.1161/STROKEAHA.111.000326. [PubMed: 23539530]

(93). Schäbitz W-R; Berger C; Kollmar R; Seitz M; Tanay E; Kiessling M; Schwab S; Sommer C Effect of Brain-Derived Neurotrophic Factor Treatment and Forced Arm Use on Functional Motor Recovery After Small Cortical Ischemia. Stroke 2004, 35 (4), 992–997. 10.1161/01.STR.0000119754.85848.0D. [PubMed: 14988579]

(94). Yu S-J; Tseng K-Y; Shen H; Harvey BK; Airavaara M; Wang Y Local Administration of AAV-BDNF to Subventricular Zone Induces Functional Recovery in Stroke Rats. PLOS ONE 2013, 8 (12), e81750. 10.1371/journal.pone.0081750. [PubMed: 24312581]

(95). Ferrer I; Krupinski J; Goutan E; Martí E; Ambrosio S; Arenas E Brain-Derived Neurotrophic Factor Reduces Cortical Cell Death by Ischemia after Middle Cerebral Artery Occlusion in the Rat. Acta Neuropathol. (Berl.) 2001, 101 (3), 229–238. 10.1007/s004010000268. [PubMed: 11307622]

(96). Lu P; Blesch A; Tuszynski MH Neurotrophism without Neurotropism: BDNF Promotes Survival but Not Growth of Lesioned Corticospinal Neurons. J. Comp. Neurol 2001, 436 (4), 456–470. 10.1002/cne.1080. [PubMed: 11447589]

(97). Stokols S; Tuszynski MH Freeze-Dried Agarose Scaffolds with Uniaxial Channels Stimulate and Guide Linear Axonal Growth Following Spinal Cord Injury. Biomaterials 2006, 27 (3), 443–451. 10.1016/j.biomaterials.2005.06.039. [PubMed: 16099032]

(98). Margulies S; Hicks R Combination Therapies for Traumatic Brain Injury: Prospective Considerations. 16.

(99). Qin Z; Joo J; Gu L; Sailor MJ Porous Films: Size Control of Porous Silicon Nanoparticles by Electrochemical Perforation Etching (Part. Part. Syst. Charact. 2/2014). Part. Part. Syst. Charact 2014, 31 (2), 171–171. 10.1002/ppsc.201470007.

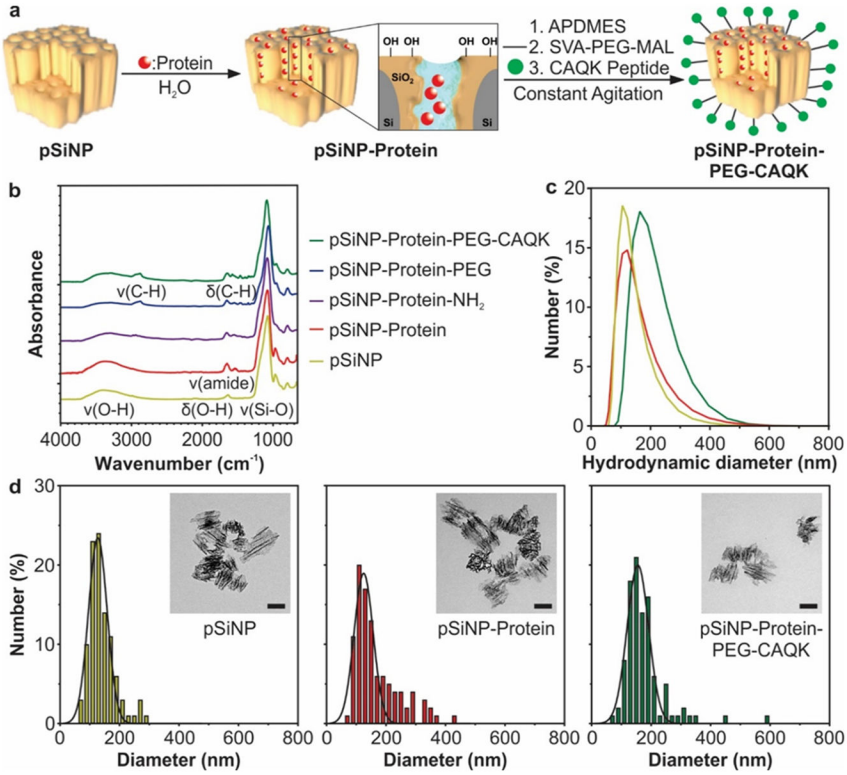


**Figure 1: Synthesis and characterization of CAQK-targeted pSiNPs encapsulating a protein cargo.**

(a) Schematic of protein loading, surface modification, and CAQK-functionalization of pSiNPs. (b) FTIR analysis of pSiNPs during synthesis steps. Nanoparticle diameters as measured by (c) DLS and (d) TEM (scale bar in inset = 100 nm).

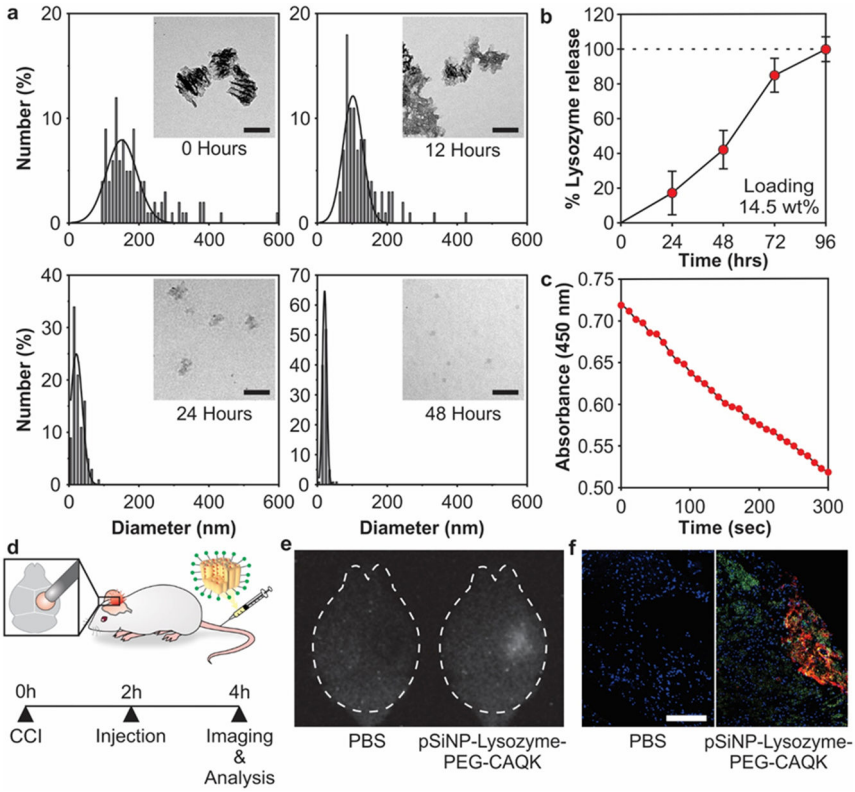


**Figure 2: Loading and biodistribution of model protein in pSiNPs.**

(a) Analysis of pSiNP-Lysozyme-PEG-CAQK size by TEM image analysis after degradation in PBS at 37 °C after 0, 12, 24, and 48 hours (scale bar = 100 nm). (b) Time-dependent release of model protein lysozyme from pSiNPs in PBS at 37 °C, measured by BCA assay. The mass percentage loading of lysozyme in the pSiNP constructs was 14.5% by mass relative to the pSiNP-protein construct. (c) Activity of lysozyme after release from pSiNPs. Lysozyme activity was assayed through the hydrolysis of Micrococcus lysodeikticus, measured by loss of absorbance at 450 nm. (d) Schematic depiction of the protocol followed in the biodistribution study. The right hemisphere was injured, followed by intravenous administration of pSiNP-Lysozyme-PEG-CAQK 2 hours post-CCI, and brains collection for downstream imaging and analysis 2 hours post-injection. (e) Time-gated image of pSiNPs in whole brains and (f) confocal image of lysozyme model protein (red), CAQK (green), and nuclei (blue) from injured brain sections (scale bar = 200 μm).

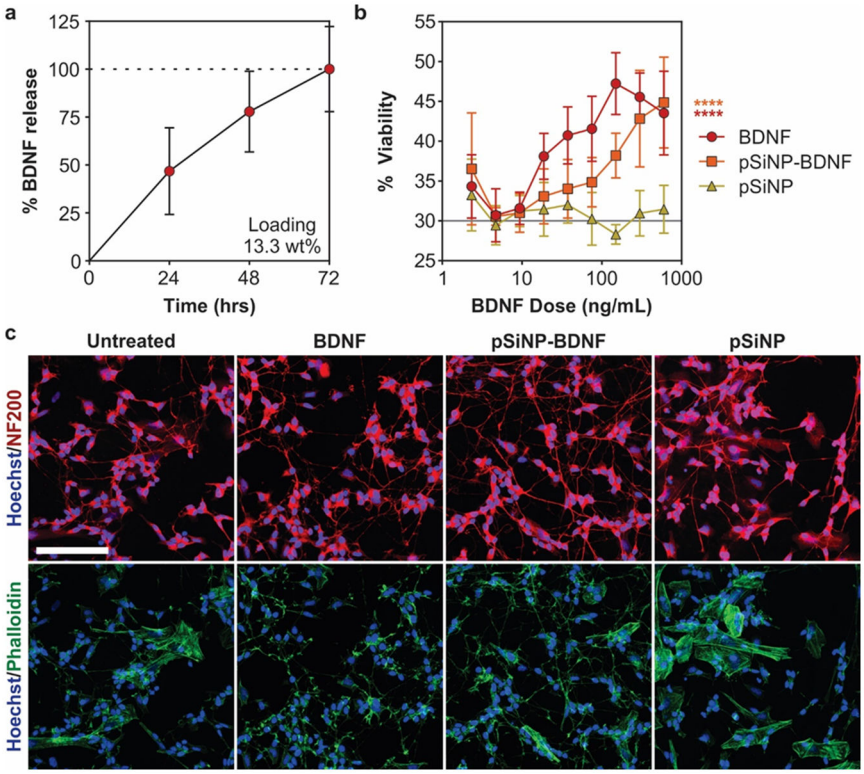


**Figure 3: BDNF loading and activity in differentiated SH-SY5Y cultures.**

(a) Time-dependent release of BDNF from pSiNPs in PBS buffer at 37 °C, quantified by ELISA. The loading of BDNF in the pSiNPs was 13.3% by mass relative to the pSiNP-protein construct. (b) Cell viability in retinoic acid-differentiated SH-SY5Y cultures treated with BDNF, pSiNP, and pSiNP-BDNF. The “pSiNP" control trace corresponds to a concentration of pSiNPs that is the same amount of Si by mass as was used in the pSiNP-BDNF formulation; *i.e.*, each point in the pSiNP control trace corresponds to a mass/volume of empty pSiNPs that is ~7.5x the ng/mL value indicated on the x-axis. (Gray line represents untreated cells; n=6, mean ± SD, **** $p \leq 0.0001$ Two-way ANOVA with Dunnett's post-test compared to pSiNP control). (c) Representative images of SH-SY5Y cells treated for 72 hours with matched concentrations of 300 ng/mL BDNF and stained with NF200 (red), phalloidin (green), and Hoechst (blue) (scale bar =100 μm).

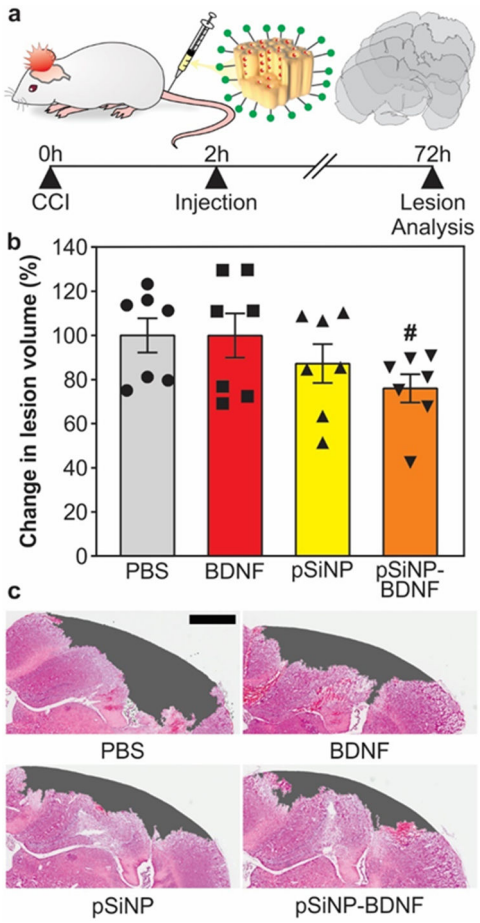


**Figure 4: Lesion volume decreases after pSiNP-BDNF treatment.**

(a) Schematic and timeline of injury, treatment, and lesion volume analysis. (b) Changes in lesion volumes relative to PBS-treated controls. (n = 7 per group, mean ± SEM, # p = 0.13 One-way ANOVA with Dunnett's post-test compared to PBS control). Both pSiNP and pSiNP-BDNF formulations contained PEG-CAQK surface chemistry as described in the text. (c) Representative images of H&E-stained coronal brain sections at 1.5 mm caudal from bregma for each treatment group with measured lesion area filled in gray (scale bar = 1 mm).